

Extracellular Calcium Transients at Single Excitations in Rabbit Atrium Measured with Tetramethylmurexide

DONALD W. HILGEMANN

From the Department of Physiology, American Heart Association Greater Los Angeles Affiliate Cardiovascular Research Laboratory, University of California, Los Angeles Center for the Health Sciences, Los Angeles, California 90024

ABSTRACT Extracellular calcium transients were resolved within the time course of single contraction cycles in rabbit left atrium using tetramethylmurexide (2 mM) as the calcium-sensitive dye (150–250 μM total calcium, 80–150 μM free calcium). Net extracellular calcium depletion began within 2–4 ms upon excitation; over the following 5–20 ms, depletion continued steeply and amounted to 0.2 $\mu\text{mol/kg}$ wet weight \cdot 10 ms (135 μM free extracellular calcium). In regularly excited muscles (0.5–2 Hz), net depletion slowed rapidly and stopped early during the rise of contractile motion monitored by transmitted light. Maximum depletions amounted to 0.2–0.5% of total extracellular calcium (0.2–0.5 $\mu\text{mol/kg}$ wet weight with 135 μM free calcium). Replenishment of extracellular calcium began at the latest midway to the peak of the motion signal. Calcium replenishment could be complete for the most part by an early phase of relaxation or could take place continuously through relaxation. The maximal net depletion per beat decreased manifold with a decrease of frequency from 1 to 0.05 Hz. During paired pulse stimulation (200–300-ms twin pulse separation at basal rates of 0.3–1 Hz), extracellular calcium accumulation was enhanced at the initial potentiated contraction; extracellular calcium depletion was prolonged at the low-level premature contraction. With quadruple stimulation (three premature excitations), the apparent rate of net extracellular calcium accumulation at potentiated contractions approached or exceeded the apparent rate of early net calcium depletion. Under the special circumstance of a strongly potentiated post-stimulatory contraction after >5 s rest, repolarization beyond -40 mV occurred within 10 ms, net extracellular calcium accumulation began with the onset of muscle motion, and net extracellular calcium accumulation (1–3 $\mu\text{M/kg}$ wet weight) coincided with a more positive late action potential in comparison with subsequent action potentials. Consistent changes of the apparent rate of early net calcium depletion were not found with any of the stimulation patterns examined. In ryanodine-pretreated atria, the duration of depletion was clearly limited by action potential duration at post-rest stimulations; in the presence of 4-aminopyridine (2 mM), depletion continued essentially undiminished for up to 200 ms. The resulting net depletion magnitudes were >10 times larger than the transient depletions found during steady stimulation.

INTRODUCTION

High temporal resolution of trans-sarcolemmal calcium movements in mammalian cardiac muscle should contribute substantially to an understanding of sarcolemmal mechanisms in the control of excitation-contraction coupling. In addition to the resolution of extracellular calcium transients during steady stimulation, this study will concentrate on intrinsic inotropic mechanisms revealed by non-steady state stimulation. The most basic phenomenon is "frequency inotropy" or an increase of force with an increase of frequency (Bowditch, 1871). With confidence, it can only be generalized at present that heterogeneous mechanisms are involved in different preparations and under different conditions. Mechanisms that must be considered on the basis of recent work are a primary accumulation of calcium at a release site (Fabiato, 1985*b*), accumulation of intracellular sodium coupled to calcium (Cohen et al., 1982), action potential broadening caused by the decay of outward current (Boyett, 1981), and facilitation of calcium current (Noble and Shimoni, 1981; Brown et al., 1984). In extracellular calcium transients, net calcium depletion during post-rest stimulation is likely to be indicative of calcium store loading. In principle, the extracellular calcium transients should reveal whether an enhanced calcium influx with an increase of frequency (see Winegrad and Shanes, 1962, and Grossman and Furchgott, 1964, for early work in atrial muscle) is due simply to a prolongation of the action potential, which would probably be reflected in the duration of influx, or to a change of calcium channel conductance, which would be reflected in the rate of depletion.

The production and decay of post-stimulatory potentiation is a striking means of directing trans-sarcolemmal calcium movements either as net calcium influx or efflux and thereby studying the underlying control mechanisms (Hilgemann, 1986). A related phenomenon of general interest in cardiac physiology is the inotropic pattern induced by paired pulse stimulation (see Cranefield and Hoffman, 1968), whereby an early, premature stimulation is imposed at short intervals after each regular excitation. During continuous paired pacing, the initial contraction becomes strongly potentiated, whereas the contractile response at the premature excitation is usually small and in some preparations can be negligible. Recently, Fabiato (1985*b*) has reproduced the inotropic patterns of post-stimulatory potentiation and paired pacing in skinned cardiac Purkinje cells with "simulated calcium currents" in calcium release experiments. This work strongly implicates the loading and release function of sarcoplasmic reticulum in these phenomena, and suggests an integration of sarcolemmal mechanisms with the calcium store function, which would generate the inotropic patterns. It should be of interest, therefore, to compare the simulated sarcolemmal function with trans-sarcolemmal calcium movements in an intact muscle during the same patterns.

A primary methodological question in this work is whether extracellular calcium transients can be confidently resolved from light changes caused by muscle contraction. In the present application, the contraction artifact (or motion signal) might be a more severe problem than in frog myocardium (Cleeman et al., 1984; Hilgemann and Langer, 1984*a*), where a direct influx of calcium from

the extracellular space may account for activation of the contraction (Antoni et al., 1969; Kavalier, 1974; Anderson et al., 1977; Morad et al., 1983). In frog ventricle, a movement compensation procedure has been described, whereby the movement artifact signals are first suppressed by a scaling and subtraction of signals without dye in the extracellular space (Cleeman et al., 1984). The wavelength-dependent light changes, which develop upon addition of dye, can then be attributed to extracellular calcium shifts. In the present work, an additional control is used, whereby the calcium-dependent signal components are suppressed with a competing calcium buffer at a high concentration. In this way, the motion artifact signals can be studied in the presence of the dye in the extracellular space. This control is important, particularly with high dye concentrations, because muscle expansion and movement might be expected to shift dye out of or into the light path. The subtraction procedure used here would exclude the influence of such an artifact by establishing that the motion signals at the wavelengths used for subtraction can be superimposed in the presence of dye on a routine basis. The approach does not depend on specific assumptions about the genesis of motion artifact signals, and it provides an independent means to select scaling factors for movement subtraction.

METHODS

The experimental set-up and muscle preparation were the same as described in the preceding article (Hilgemann, 1986). In order to achieve a nearly homogeneous excitation of the patch of muscle in the light path, field stimulation was applied via platinum wire electrodes mounted just outside the 1.5-mm fiber optic used for illumination. With the chosen electrode configuration and the stimulation strength set at 2.5 times threshold (0.5 ms), the upstrokes of action potentials measured at various positions in the muscle preparation were usually <2 ms out of phase. From the falling edge of the stimulus, the time to peak of action potentials measured in the illuminated muscle patch was routinely 2–3 ms; at low frequencies of excitation, which correspond to short, spike-like action potentials in this preparation, times of 3–5 ms were obtained. Action potentials were measured either before or after optical measurements. Absolute potential calibrations have not been given in the figures because of the relatively long duration of many impalements and the resulting baseline drift using the floating electrode arrangement. In those cases where the absolute potential was of special importance, short-term impalements were made with multiple checks of the resting membrane potential. The individual light signals were low-pass-filtered at 5 kHz and acquired digitally at 6–20 kHz using a Cromemco 3 (Mountain View, CA) microcomputer with 12-bit analog-to-digital conversion. To obtain satisfactorily low noise levels at the wavelengths with high background absorbance, 5–50 acquisitions were averaged for the signals presented.

The bath solution composition was (mM): 145 Na⁺, 138 Cl⁻, 2.5 K⁺, 0.5 Mg⁺⁺, 15 dextrose, 20 HEPES, pH 7.3; calcium concentrations are given in the text and figures. The citrate-containing bath solution had the following composition (mM): 145 Na⁺, 35 Cl⁻, 2.5 K⁺, 30 citrate, 7 total calcium (or as given in text), 15 dextrose, 50 sucrose to maintain osmolarity, 20 HEPES, pH 7.3. Magnesium was not added since it would have been bound. In some experiments, magnesium was also omitted from the normal bath solution as a control, but this factor had no effect on the results obtained in this preparation. The total calcium concentration of the citrate solution was chosen empirically to result in contraction artifacts of nearly the same magnitude as in the normal dye-containing solution (usually 120 μM free calcium). The free calcium of a 30 mM citrate-

containing bath solution with 7 mM total calcium was estimated at 160 μM with a calcium electrode. The free calcium concentrations of citrate solutions, which resulted in an equivalent contractility to normal bath solution, were consistently 25–40% higher than the normal bath solution. The same discrepancy was found when high concentrations of malate were used to buffer free calcium at higher concentrations. It is difficult to eliminate entirely the effects of anion substitution on the calcium electrode as a contributing factor (Dani et al., 1983), but it is striking that extracellular calcium buffering did not increase contractility in any observation. The citrate-containing solution had no discernible deleterious effects on muscle function or excitability and did not change the basic contractile responses during non-steady state stimulation.

The motion artifact signals corresponded to a decrease of absorbance in the large majority of rabbit atrial preparations. The peak magnitude of motion artifacts correlated closely with the peak developed tension over the range of contractility changes occurring in this study. Fig. 1 describes the typical relationship found between the two signals under the conditions of experiments (200 μM total calcium, 2 mM tetramethylurexide), representative of >20 observations. Fig. 1A shows averaged tension and light signals (680-nm signal) during steady 1 Hz stimulation (1), during 4 Hz stimulation (2), and at the subsequent potentiated post-stimulatory contraction after a 5-s pause (3). The signals at 1 Hz were scaled to the same magnitude, and the relative magnitudes of the two signals at the lower and higher levels of contractility fall within 15% of one another. As can be seen here, the magnitudes of the contraction artifacts were found to rise and fall a bit more steeply than in the tension response during these contractility changes. However, the differences were consistently so minor that separate acquisition of a motion signal and the tension signal did not seem to be warranted for routine purposes.

The 680-nm motion artifact signal is used in this study as a monitor of the contractile response, primarily because it is the relevant control of contractility for the other light signals. A second reason for this choice is given in Fig. 1B, which shows the averaged 680-nm light signal and developed tension at 1 Hz stimulation from another muscle (same conditions). The light signal (680 nm) has a waveform somewhat different from that of the tension signal. Although this discrepancy was not invariable, the optical latency period at low levels of contractility was often significantly shorter than the mechanical latency period. For this work, the implication is that the contractile event can impinge on the resolution of the extracellular calcium transient at an earlier time than suspected from a tension record.

Fig. 2 places the contractile state of muscles during extracellular calcium transients (200 μM total calcium, 120 μM free calcium) in relation to the midrange of contractility for a muscle. Tension measurements are shown in A for a post-stimulatory potentiation sequence and in B for steady state contractions at 2 Hz under the conditions of extracellular calcium transients. Part C shows steady state contractions at 2 Hz with 2 mM calcium (no dye); the contraction magnitude could be increased an additional 1.8-fold by increasing the bath calcium to 6 mM. It should be kept in mind, therefore, that the maximum contraction occurring in this study in extracellular calcium transients is not more than 12% of the peak contraction magnitude obtainable with high calcium.

The precise forms and time courses of contraction artifacts at the different wavelengths monitored are of critical importance for this work. In previous studies, which examined net extracellular calcium shifts during non-steady state stimulation, all preparations selected for homogeneity could be used. However, a more stringent criterion was necessary in the present work. The criterion for results presented here was that motion artifact signals could be superimposed after suppression of the calcium-dependent component in the citrate solution. If this was not the case, the muscle was repositioned in the chamber and the motion artifacts were examined again. If wavelength-independent motion artifacts

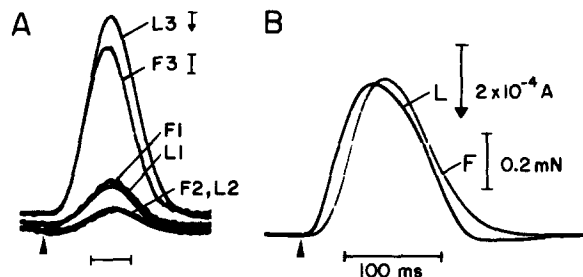


FIGURE 1. Signals marked "L" are motion artifact signals at 680 nm; an upward swing of the signal corresponds to a decrease of absorbance. In this and the other figures, the direction of the arrows used to calibrate the light signals gives the direction of increasing absorbance; stimulations are marked by arrowheads. Signals marked "F" are the corresponding tension responses. 200 μ M total calcium, 2 mM tetramethylmurexide. Part A shows the averaged light and tension responses during the post-stimulation potentiation sequences. F1 and F2 are steady state signals at 1 Hz; L2 and F2 are during 4 Hz stimulation; L3 and F3 are the signals found at post-stimulatory excitation after a 5-s pause. The signal baselines were separated for a clearer presentation. Part B shows the averaged light (L) and tension (F) responses of a different muscle stimulated continuously at 1 Hz. Note that the light signal is displaced to a somewhat earlier time course than the tension signal. Calibration bars given in B also apply to the bars given in A. See text for details.

were not obtained in three or four attempts, the muscle was discarded. Stable, wavelength-independent motion artifacts could be achieved in $\sim 30\%$ of the muscles. The following comments represent the experience of the author with more than 100 rabbit atrial preparations used to resolve extracellular calcium transients at high temporal resolution.

In a large percentage of muscles ($\sim 50\%$), the 470- and 580-nm signals could be superimposed or very nearly superimposed by scaling, but the 680-nm signal showed discrepancies in the exact time course of either the rising or falling contraction phase. This finding is not surprising, given the possibility that shifts of dye into or out of the light path could contribute to the motion artifact signals. In this respect, the choice of 470- and 580-nm signals is advantageous for subtraction of the motion artifacts, since the

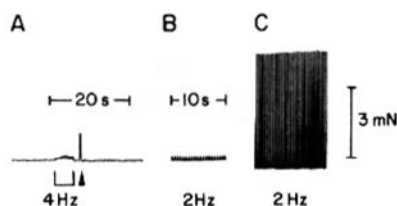


FIGURE 2. Tension responses of a muscle under the conditions of extracellular calcium transients (parts A and B: 200 μ M total calcium, 2 mM tetramethylmurexide) and at 2 mM calcium (part C: no dye). Part A shows a post-stimulatory potentiation sequence: 4 Hz stimulation for 8 s, 2 s rest, and a single post-stimulatory excitation marked by an arrowhead. Part B shows the contractions obtained during continuous 2 Hz stimulation. Part C shows the contractions obtained at 2 Hz after washout of dye and incubation with 2 mM calcium (same time scale as in part B).

baseline absorbances of tetramethylmurexide are nearly identical at these wavelengths with the calcium concentrations used (150–250 μM total calcium). This consideration is an advantage of tetramethylmurexide over antipyrylazo III, which requires subtraction of signals at wavelengths with very different baseline absorbances. The subtraction of narrowly spaced wavelengths in a calcium-sensitive wavelength range of the tetramethylmurexide spectrum also is subject to this problem; if dye shifts out of or into the light path, artifacts of different magnitude at different wavelengths would occur because of the different background absorbances. Furthermore, measurement of wavelengths with extremely high absorbances would have been necessary on a routine basis (500–550 nm). For example, >100 averagings of the isobestic point (510 nm) were necessary to obtain reasonably low noise levels even in the ryanodine state; in three of three observations, 510 nm behaved in a completely calcium-independent fashion. Most importantly, a routine subtraction of narrowly spaced wavelengths was not reasonable, because the resulting calcium-dependent signals are of small magnitude in relation to the movement signal. The opposite calcium-dependent absorbance shifts at 470 and 580 nm give the largest possible ratios of calcium-related to movement-related signals.

In ~25% of the muscles, the 580- and 470-nm signals could not be superimposed by scaling. Rarely, large discrepancies were found, including the possibilities of biphasic motion artifacts and motion artifacts of different sign. Systematic deviations at the different wavelengths could not be established. In the large majority of preparations, the magnitudes of motion artifacts at 580 and 470 nm, in the presence of dye, were within 25% of one another. In the majority of experiments, motion artifacts at 680 nm were of somewhat larger magnitude than artifacts at lower wavelengths. In other types of preparations studied (e.g., guinea pig atrium), these generalizations do not hold, although very similar extracellular calcium transients have been obtained. The adjustments of scaling factors needed to superimpose the 580- and 470-nm signals presented in this article were not more than 15% from scaling by transmitted light intensity. The calibrations given for the subtracted signals are a mean of the calibrations at the individual wavelengths. Essentially identical extracellular calcium transients were obtained when the motion artifacts reflected a decrease or increase of absorbance. One example of positive motion artifacts is given in the Results.

Significant calcium buffering by fixed binding sites in the extracellular space could influence both the magnitude and kinetics of extracellular calcium transients. Also, electrostatic interactions of calcium and/or dye with the cell surface might be expected to play a role in fast signals. Up to now it can be noted, however, that several relevant interventions did not alter any qualitative or temporal aspect of the signals described. (a) Extracellular acidosis has been found to effectively decrease the lanthanum-displaceable calcium fraction found in cardiac tissue culture and gas-dissected membrane preparations (Langer, 1985), which probably reflects calcium bound to sarcolemmal membranes (Langer, 1984). A reduction of the bath solution pH from 7.3 to 6.5 resulted in a threefold shift of the threshold for stimulation, but only decreased the magnitude of signals obtained (~30%) without any change of their kinetic characteristics. (b) Dimethonium is a positively charged divalent molecule, which should screen calcium from the so-called diffuse double layers and reduce the magnitude of the layer at high concentrations (McLaughlin et al., 1983). No effect was found at concentrations up to 10 mM, and at concentrations up to 20 mM the threshold for stimulation was shifted to higher values but extracellular calcium transients were only decreased slightly in magnitude. (c) Magnesium in concentrations up to 10 mM, 80 times higher than the free calcium concentration in experiments, also had no effect on the time courses of signals obtained, and depressed the initial rates of calcium depletion by not more than 25%.

RESULTS

Extracellular Calcium Transients During Steady State Stimulation

The ratio of calcium-dependent to contraction-dependent light signal components clearly improved with a reduction of extracellular calcium (or other negative inotropic interventions). This is because the magnitudes of movement artifact signals were clearly a relatively steep function of the extracellular calcium concentration, whereas the magnitude of the extracellular calcium transients increased roughly linearly with increasing calcium over the range of 50–300 μM . At 300 μM total calcium, however, resolution of extracellular calcium transients from the motion artifact signals was difficult. Therefore, most work was carried out with 150–250 μM total calcium. The relevance of the signals presented here to excitation-contraction coupling at normal calcium concentrations is supported by the ability to evoke characteristic contractile responses to premature or rapid stimulation and paired pulsing, contractile patterns widely thought to reflect the release of calcium by an internal calcium store. At lower total calcium concentrations of 40–80 μM (25–50 μM free calcium), it was possible to evoke cumulative depletions of extracellular calcium with almost no contractile response, but the typical contractile patterns were absent (and with time preparations became inexcitable). Correspondingly, post-stimulatory excitations did not result in potentiated contractions or net accumulation of extracellular calcium as described previously (Hilgemann, 1986). In this work, as well as in work with other preparations (primarily frog ventricle and guinea pig atrium), slow positive staircase mechanisms, taking 2–6 min to accumulate at normal calcium, were often of very small relative magnitude, although muscles responded strongly to other positive inotropic interventions (e.g., isoproterenol).

Figs. 3 and 4 present signals obtained during steady stimulation at 2 Hz with 0.25 and 0.1 mM total calcium, respectively. Fig. 3 demonstrates the movement subtraction procedure for the worst ratio of movement signal to calcium signal in this article, and this is the most extreme situation where the movement subtraction procedure would be defended as giving an accurate representation of the extracellular calcium transient. Parts *A* and *B* of Fig. 3 show signals obtained in the citrate containing solution (30 mM citrate, 7 mM total calcium); *C* and *D* show signals without citrate (250 μM total calcium, 135 μM free calcium). Part *A* shows the raw signals with scaling factors adjusted so that the three light signals are superimposable. The scaling factors for the 580- and 470-nm signals are within 15% of scaling by transmitted light intensity and are the same in each part of the figure; the scaling factor for the 680-nm signal is smaller, reflecting a larger motion artifact at 680 nm.

Fig. 3*B* shows the inverted 680-nm signal and the 470–580-nm subtracted signal (i.e., the 580-nm signal subtracted from the 470-nm signal, hereafter referred to as the 470–580 signal) after amplification of each of the signals by a factor of 2. The subtracted signal is nearly flat at this amplification. Part *C* shows the raw light signals with the normal bath solution (same calibrations as in *A*). Note that there is an initial increase of absorbance at 580, a decrease at 470 nm, and no change at 680 nm during the latency period. In this example, the slopes

of the initial absorbance changes are considerably less than the slopes of absorbance changes during contraction (compare Fig. 4). Part *D* (no citrate) shows the inverted 680 motion artifact and the 470–580 signal, at the same amplifications as in part *C* with citrate. This signal is the best estimate of the extracellular calcium transient. Part *D* also gives the action potential measured after the data acquisition period.

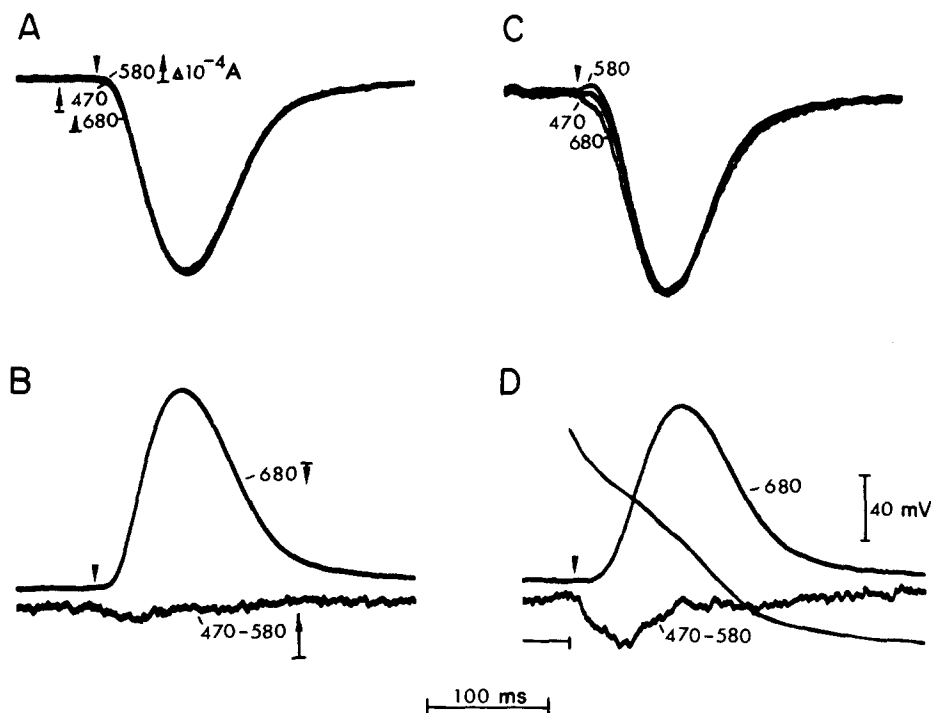


FIGURE 3. Movement subtraction procedure for 2 Hz stimulation. 250 μ M total calcium, 2 mM tetramethylmurexide. Parts *A* and *B* show the signals obtained in the 30 mM citrate/9 mM total calcium solution; *C* and *D* are without citrate. *A* and *C* are raw signals, scaled to superimpose in *A*; *B* and *D* show the inverted 680-nm motion artifact signals and the 470–580-nm signals from *A* and *C*, respectively. The calibration arrows give the direction of increasing absorbance. Calibrations are the same in *A* and *C*, and in *B* and *D*. The best estimate of the extracellular calcium transient is the 470–580 signal given in part *D*, which also shows the corresponding action potential. See text for complete details.

The assumption underlying this subtraction procedure is that the high citrate concentration would buffer calcium fast enough and efficiently enough to greatly limit calcium movement to and from the 2 mM tetramethylmurexide. This assumption is clearly supported by the nearly complete abolition of fast light changes, which are consistent with an initial depletion of extracellular calcium in these experiments. The assumption is also supported by the fact that the initial light changes interpreted as calcium depletion could be very markedly reduced

with less extensive buffering (8 mM citrate). The time courses of light signal changes upon switching solutions were consistent with an excess citrate buffer capacity; signals interpreted as calcium depletion disappeared within 1–2 min upon switching to the citrate bath solution, whereas 6–15 min was required for the signals to return after switching back to the normal bath solution. At both 470 and 580 nm, baseline absorbances of the dye in the two solutions were not more than 15% discrepant. Motion artifact signal magnitudes were nearly identical in the two solutions.

The subtracted signal reflects an early, rapid depletion of extracellular calcium, which, however, slows markedly by the initial rise of motion and stops early in the rising motion signal. A slowing of the absorbance shifts, thought to represent net calcium depletion, is actually apparent in the latency period of the raw signals on close examination. Replenishment of extracellular calcium is essentially complete by the end of the contraction, and is complete to a substantial degree by the peak of contraction. The magnitude of depletion is estimated at $0.6 \mu\text{M}$ of the total $250 \mu\text{M}$ extracellular calcium ($150 \mu\text{M}$ free calcium). With motion signals of this magnitude, the putative extracellular calcium transient can be changed markedly by the scaling procedure, which can either accelerate or slow the replenishment phase. The rapid depletion phase can be extended or abbreviated within a factor of ~ 2 before obvious effects of muscle contraction are apparent in the subtracted signal (15–20% changes of the scaling factors). However, the initial rate of calcium depletion over the first 15–20 ms ($\sim 0.5 \mu\text{M}/10 \text{ ms}$) is not dependent on the scaling procedure, nor is the conclusion that extracellular calcium re-equilibrates to the prestimulatory level by the end of contraction. The inferred rate of calcium influx would be $0.2 \mu\text{mol}/\text{kg wet weight} \cdot 10 \text{ ms}$ (40% extracellular space). Here and in all subsequent references to rates, tangent lines to the extracellular calcium transients were drawn by eye and the slopes were calculated from calibrations of the signals or derivatives were calculated from second-order polynomials fitted to 20 points.

Fig. 4 shows the more advantageous situation, which can be achieved routinely with $100 \mu\text{M}$ total calcium (2 Hz stimulation). In this one case, signals are presented with a positive contraction artifact component. Part A shows the raw, intensity-scaled signals; total light changes in these signals are much smaller than in the previous figure; the 470- and 580-nm signals show more noise owing to the high background absorbance of the dye as compared with the 680-nm signal. Note the rapid fall of absorbance at 470 nm and the increase of absorbance at 580 nm. Part B of the figure shows subtracted signals, and illustrates that essentially the same extracellular calcium transient can be obtained by each of the three possible movement subtractions. For the top curve, the 680-nm signal is subtracted from the 470-nm signal. For the middle curve, the 680-nm signal is subtracted from the 580-nm signal, and the inverted signal thought to reflect extracellular calcium has been amplified by a factor of 1.3 to give a signal of similar magnitude to the previous one. The bottom signal given is the usual 470–580-nm subtraction with the amplification decreased by a factor of 2 to make the resulting signal similar in magnitude to the others. The magnitude of the subtracted signal in this case is substantially larger than the contraction artifact

signal component at any of the wavelengths, and scaling factors can be changed by >20% with only little effect on the resulting signal (primarily a change of the apparent rate of calcium replenishment).

Fig. 4C shows the 680-nm motion signal at high amplification and the best estimate of the extracellular calcium transient (470–580 nm). Note the rather short optical latency period. With confidence it can be reported that the steep

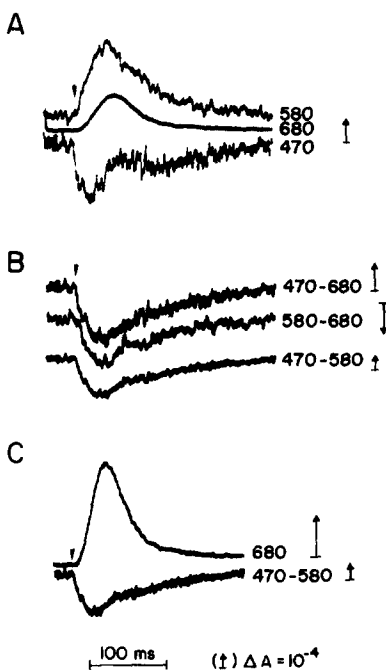


FIGURE 4. Signals obtained with 2 Hz stimulation at 100 μ M total calcium. The contraction artifact corresponds to an increase of absorbance (single example in this article). Part A shows the raw signals, scaled by transmitted light intensity. Note the large magnitude of initial absorbance shifts at excitation in relation to the 680-nm motion artifact signal. Part B shows the three possible subtractions of these signals, resulting in essentially the same extracellular calcium transient. The subtracted signals have been amplified appropriately to give signals of similar magnitude (see calibration bars). Part C shows the amplified 680-nm signal with the best estimate of the extracellular calcium transient (470–580-nm subtraction). See text for further details.

depletion phase began within 4 ms of stimulation in this muscle and in the great majority of preparations studied; this was determined from differentiated signals. The onset of depletion could often be accelerated by increasing the stimulation parameters. Therefore, a more detailed analysis of the onset of depletion did not seem useful. In comparison with Fig. 3, the depletion continued almost linearly into the motion signal and stopped about one-third of the way to motion peak. Replenishment takes place through the motion signal and continues into a slow terminal relaxation phase, which is apparent in the amplified motion artifact

signal. The late re-equilibration of extracellular calcium can be inferred from the raw 470- and 580-nm light signals, which show relatively slow, opposite changes through the terminal relaxation phase. The total magnitude of depletion is estimated at $0.4 \mu\text{M}$ of the $100 \mu\text{M}$ total extracellular calcium.

Frequency of Stimulation

All subsequent extracellular calcium transients were made using 150 or $200 \mu\text{M}$ total calcium, concentrations at which the primary interval-strength mechanisms of interest were invariable, and at which resolution of the calcium transient was not severely limited by motion signals. Fig. 5 shows typical motion signals and extracellular calcium transients determined at three frequencies ($200 \mu\text{M}$ total calcium). In this case, the signals were obtained in the presence of $1 \mu\text{M}$ propranolol to avoid possible effects of catecholamine release. The signals labeled "1" were at 0.02 Hz stimulation, those labeled "2" were at 0.3 Hz, and those

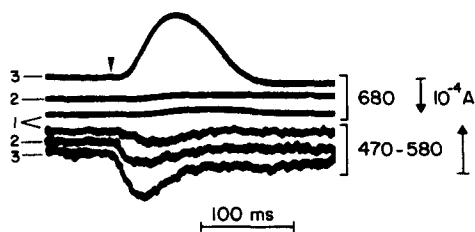


FIGURE 5. Extracellular calcium transients and 680-nm motion artifact signals obtained at 0.02 (1), 0.3 (2), and 1.0 (3) Hz. $200 \mu\text{M}$ total calcium. Scaling factors determined for the 1.0 -Hz signals were applied to the other two sets of signals.

labeled "3" were at 1.0 Hz. The scaling factors used in all of the signals were those obtained for subtraction of the contraction artifact at 1.0 Hz. The maximum net depletion at 0.02 Hz was at least fivefold smaller than at 1.0 Hz, which was typical for 10 observations. At 0.3 Hz, a rapid initial depletion was apparent, and at 1.0 Hz the depletion was somewhat prolonged to ~ 25 ms (see also Fig. 7 regarding prolongation); replenishment of calcium was not complete within the time course of the contraction. A close examination of the signals reveals at most a modest increase of the initial rate of depletion in the signal at 1.0 Hz in comparison with the signal at 0.3 Hz. The almost complete absence of an extracellular calcium signal at 0.02 Hz is striking, but 0.5 – 1.5 mM 4-aminopyridine (4-AP) invariably increased the extracellular depletion at low frequencies to nearly the magnitude and speed of those found at high frequencies; in the presence of 1 mM 4-AP, an enhancement of net depletion with an increase of frequency was found in only 2 of 12 preparations studied (for brevity, no curves are presented; further relevant results are given in subsequent figures). Facilitation of depletion responses was not found in guinea pig atrium or frog ventricle.

Extracellular Calcium Transients During Paired Pulse Stimulation

Figs. 6–8 present extracellular calcium transients obtained during continuous paired pulse stimulation that are representative of >30 observations. For the

signals described in Fig. 6 (150 μM total calcium), twin stimulations were applied at 200-ms intervals at a basal rate of 0.5 Hz. Panel *A* shows the raw light signals with the scaling factors used to resolve the extracellular calcium transient, which is shown in *B*, together with the inverted 680-nm contraction artifact signal. The motion artifacts reflect the usual contractile pattern during paired pulse stimulation in this preparation, the initial contraction being of large magnitude and the premature contraction being of very small magnitude. The raw signals (*A*) have been arranged so that the signals join at the premature stimulation. At that point, the increasing absorbance at 580 nm, the decreasing absorbance at 470

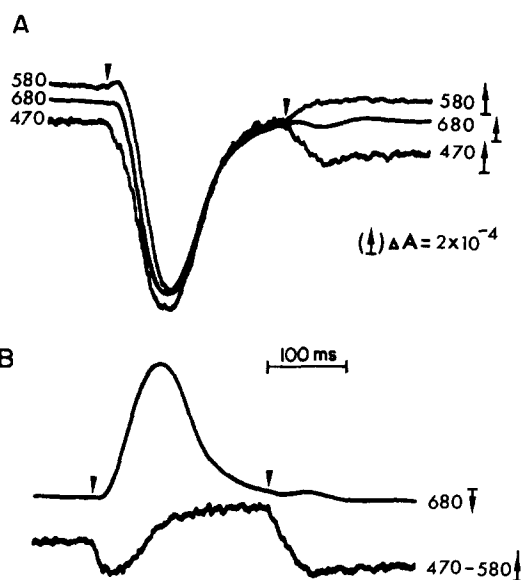


FIGURE 6. Paired pulse stimulation. 200-ms intervals, 0.5 Hz basal frequency, 150 μM total calcium. Part *A* shows raw signals with scaling factors chosen by the subtraction procedure. Part *B* shows the inverted 680 motion artifact signal and the 470–580 signal, which is the best estimate of the extracellular calcium treatment. See text for further details.

nm, and the lack of change at 680 nm are indicative of a net depletion of extracellular calcium with almost no contractile response. The total magnitude of absorbance shifts at the premature excitation (470–580 nm) was typically $\sim 20\%$ of the magnitude of contraction artifacts at the initial excitation. With 150 μM total calcium, the 470- and 580-nm signals obtained in citrate bath solution could be superimposed routinely at basal frequencies of up to 1 Hz. For brevity, citrate signals will be shown only for the more extreme case of three premature excitations described later.

The following features of the subtracted signal are not dependent on the precise subtraction procedure: (*a*) the apparent early rates of depletion are very similar at the initial and the premature excitations; early signals can be superimposed within their signal width; (*b*) the first excitation results in net extracel-

lular calcium accumulation; (c) the premature excitation results in a prolonged period of net depletion through the peak of the small motion artifact signal. As with previous signals, the aspect that is most sensitive to the subtraction procedure is the time course of calcium efflux during contraction, which can be made to appear complete at about the peak of contraction or can take place more slowly up to the premature excitation. In the majority of experiments, the controls favored a scaling of the subtracted signal, with the steepest portion of calcium accumulation falling about one-third of the way to the peak of contraction. The net calcium depletion at the premature excitation, which was unaffected by large changes of the scaling factors, is estimated at $1.2 \mu\text{M}$ of the total $150 \mu\text{M}$ extracellular calcium. Note that the subtracted signal underwent a downward

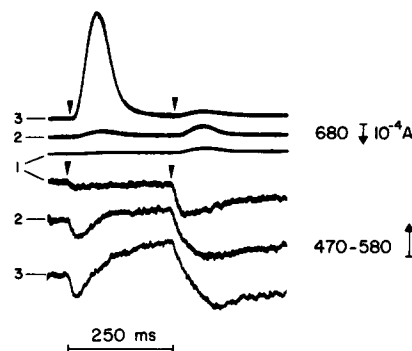


FIGURE 7. Effect of basal frequency on paired pulse stimulation. 250-ms intervals, $150 \mu\text{M}$ total calcium. The upper three signals are 680-nm motion artifact signals; the lower three signals are the 470–580-nm signals. Signals marked 1 are at 0.02 Hz; those marked 2 are at 0.3 Hz; those marked 3 are at 0.6 Hz. See text for further details.

shift during the observation period, which is indicative of a net calcium uptake during each twin pulse sequence and net extrusion between the acquisition periods; this was typical in the great majority of observations.

Fig. 7 describes the effect of the basal stimulation rate on the paired pulse signals. In this case, the twin stimulations were made at 250-ms intervals. The basal frequencies for the signals are 0.02 (1), 0.3 (2), and 0.6 (3) Hz. The motion artifact signals are given in part A; the 470–580-nm signals, all determined with the same scaling factors, are given in part B. At the initial excitation at 0.02 Hz, depletion was close to noise level; at the subsequent premature excitation, depletion was rapid but brief, and the twin stimulation resulted in an estimated net depletion of extracellular calcium of $0.8 \mu\text{M}$. At the initial excitations, the magnitudes of both depletion and replenishment increased with an increase of the basal rate. Comparing the 0.3- and 0.6-Hz responses, the calcium accumulation phase was more strongly enhanced and accelerated at 0.6 Hz. The maximal rate of net extracellular calcium accumulation at 0.6 Hz was $\sim 70\%$ of the initial rate of calcium depletion at 0.6 Hz. The increase of the basal rate clearly increased the duration of depletion at the premature excitations; the early

depletion signals could be quite precisely superimposed after amplification and appropriate display.

Action potentials measured during paired stimulation consistently showed a rapid repolarization at the initial large contraction, with net calcium accumulation taking place through repolarization. Action potentials at premature excitations were prolonged by comparison in a positive potential range. With an increase of the basal rate, the action potentials increased in duration at both the initial excitation and the premature excitation. Under control conditions, as in Figs. 6 and 7, the transition from calcium depletion to calcium replenishment at the initial excitation was estimated to take place between -20 and -40 mV. In an

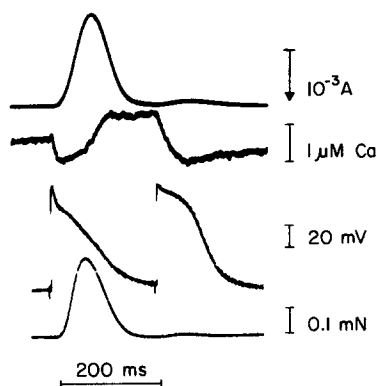


FIGURE 8. Paired pulse stimulation in the presence of 2 mM 4-AP. 200-ms intervals, 0.5 Hz basal frequency, 150 μ M total calcium. From top to bottom the signals given are: (1) 680-nm motion artifact; (2) extracellular calcium transient (470–580 signal), calibrated as a change of mean extracellular calcium; the total signal magnitude in absorbance is 2.5×10^{-4} A; (3) action potentials measured after acquisition of the light signals; (4) tension record measured with the action potentials. See text for further details.

attempt to prolong the action potential and (presumably) eliminate the influence of calcium-independent transient outward current, the signals were examined in the presence of a high concentration of 4-AP (2 mM). This concentration fully abolishes positive action potential staircases found with increments of frequency in this preparation. For the results presented in Fig. 8, action potentials were measured after the extracellular calcium transient.

Fig. 8 gives the motion signal, the extracellular calcium transient, the action potential recording, and the actual contraction record for the sequence. Notably, the initial repolarization remained quite rapid at the potentiated contraction in comparison with the premature excitation. Depletion stopped early during the rise of contraction at about -10 mV. Calcium accumulation was delayed in comparison with previous results (confirmed in five observations) and appeared to take place in two phases, becoming more rapid during the late rise of contraction and being complete before relaxation and repolarization ended. At the premature excitation, the action potential showed a genuine plateau corresponding closely to the period of net calcium depletion.

Quadruple Pacing

In Fig. 9, the paired pulse sequence is extended to three premature excitations. The movement subtraction procedure is shown for the repeated sequence of four rapid stimulations at 250-ms intervals (three premature excitations), followed by a stimulation pause of 2 s. Before acquisition of signals, the stimulation sequence was repeated until a steady state was achieved. Part A shows the signals

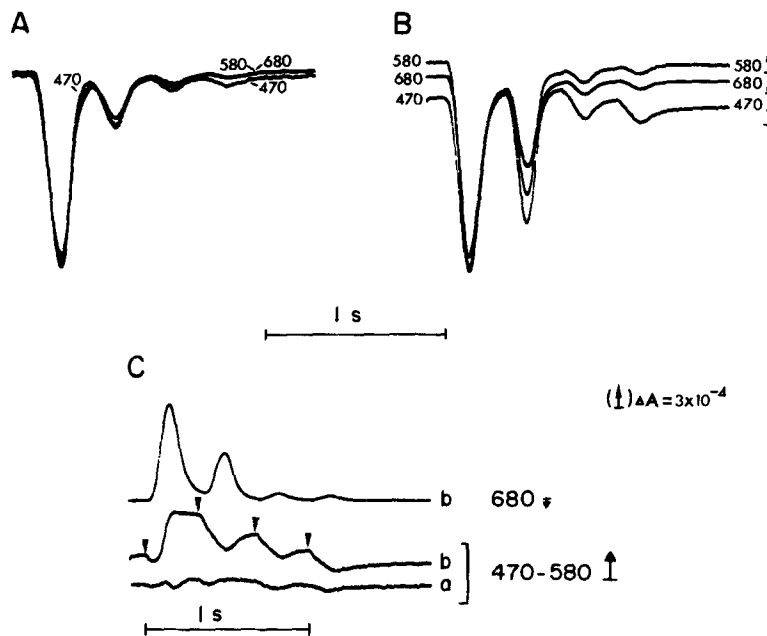


FIGURE 9. Quadruple pacing. An initial excitation is followed by three premature excitations at 250-ms intervals and a 2-s rest pause. $150 \mu\text{M}$ total calcium. (A) Light signals obtained in a 30 mM citrate/6.5 mM total calcium bath solution after adjustment of the scaling factors to superimpose the signals. (B) Signals obtained without citrate. Calibrations are given at the right of the signals, corresponding to $3 \times 10^{-4} \Delta A$. (C) Inverted 680-nm motion artifact signal (*b*) from part B; the 470–580 signal, *a*, is the subtraction of the citrate signals in A; the 470–580 signal *b* is the subtraction of the signals without citrate in B. Scaling factors for the individual wavelengths are identical in each panel of the figure, except for the 680 motion signal in C. See text for further details.

obtained in the citrate solution, with scaling factors adjusted to superimpose the signals as nearly as possible. Part B shows the signals obtained without citrate, arranged so that the signals join at the first premature excitation. Part C shows the inverted motion artifact signal (680 nm) without citrate, the 470–580 signal without citrate (*b*), and the 470–580 signal with citrate. The scaling factors for the 470- and 580-nm signals are the same throughout the figure. The amplification of the 680-nm signal was decreased somewhat in part C for spatial reasons.

The net absorbance shifts produced by the stimulation sequence (measured at the end of relaxation) are suppressed in the citrate solution by $\sim 90\%$ (compare

A and *B*, or the subtracted signals *a* and *b* in part *C*). As is apparent in Fig. 9*C*, the motion subtraction leaves some small transient shifts of absorbance, which at the potentiated contraction are probably due to incomplete movement subtraction. At the subsequent premature excitations, the residual transient absorbance shifts could be due to incomplete calcium buffering by 30 mM citrate as well as incomplete movement subtraction. The net accumulation of extracellular calcium at the first excitation was substantially larger and faster than in signals obtained for paired stimulation. The apparent rate of early depletion remained similar at each excitation, but depletion was very much abbreviated at the initial excitation. Net calcium accumulation begins with a delay of ~50 ms, and relatively small changes of the scaling factors have a large effect on the time course of accumulation. Changes of the scaling procedure in the great majority of experiments displaced the apparent calcium accumulation in time, rather than simply prolonging or shortening the time course. Although it has never been obtained in experiments, the slowest possible time course of calcium accumulation, namely a straight line from the initial small depletion to the end point of relaxation, would leave the calcium accumulation rate of a magnitude equal to that of the early depletion rate.

Two Phases of Calcium Accumulation

It was notable that in many signals obtained during paired and quadruple pacing, calcium accumulation appeared to take place in two phases, an early rapid phase during the rising motion signal and a slower phase through the rest of the contractile event. This is described in Fig. 10*A* for the quadruple pacing sequence from another experiment. At the first potentiated contraction, net calcium accumulation begins at the onset of motion, accelerates through the rising motion signal, and then continues at a slower rate through the motion signal and up to the following premature excitation. Variations of the scaling factors could have shifted the early accumulation phase to a somewhat faster time course or to a later time course, but did not abolish the late phase. In the previous figure, a substantial late phase of calcium accumulation is apparent at the second excitation in the sequence.

Fig. 10*B* shows a stimulation sequence during which a dual time course of accumulation was invariably found under conditions very favorable for resolution. The stimulation pattern is alternating intervals of 400 and 350 ms, which results in alternating large and small contractions (see the 680-nm signal). On careful examination, it can be seen that the muscle did not relax completely between stimulations. At the longer interval (larger contraction), calcium accumulation began sharply at a point early in the rising motion signal, and then slowed rather abruptly before the peak of the motion signal to a fairly constant rate up to the following excitation. At the shorter interval (smaller contraction), the rapid accumulation phase was almost absent, and accumulation through the late relaxation phase up to the next contraction took place at the slower rate. This "slow" rate, which seems to correlate with a small delayed phase of relaxation (compare also with Figs. 3 and 4), is still very much faster than the rate of re-equilibration of extracellular calcium after a cumulative depletion response, which can take several minutes (see Hilgemann, 1986).

Fig. 11 presents the time course of extracellular calcium changes at a potentiated post-stimulatory contraction, after an 8-s train of 4 Hz stimulation as described previously (Hilgemann, 1986). The stimulation sequence could not be generated by the computer program and was made by hand in 10 experiments, with control of the data acquisition for the potentiated contraction by a prepulse from the stimulation unit. Panel A shows the raw signals for the sequence: the

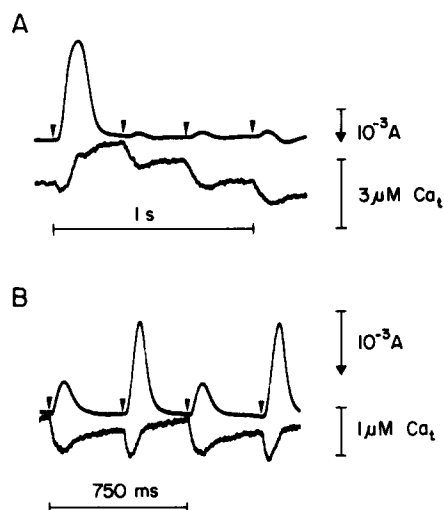


FIGURE 10. (A) Quadruple pacing sequence under conditions identical to those in Fig. 9. The extracellular calcium transient (lower signal) is calibrated in terms of mean extracellular calcium. Signals illustrate two differences from signals in Fig. 9. The rapid calcium accumulation phase at the initial excitation is followed by a slower phase through most of the contraction. The premature excitations result in smaller contractions (see upper 680-nm motion artifact signal) with only a small late efflux phase compared with Fig. 9. (B) Signals obtained with alternating 400- and 350-ms intervals. 150 μ M total calcium. The extracellular calcium transient (lower signal) is also calibrated in terms of mean extracellular calcium. Note that the larger contraction artifacts, after the 400-ms intervals, are accompanied by a rapid calcium accumulation phase. At the smaller contraction artifacts, the rapid phase is almost absent. The slow efflux phase appears to correlate with a slow terminal relaxation, apparent on close examination of the 680-nm motion signal. See text for further details.

muscle was stimulated at ~ 0.1 Hz, and then at 4 Hz for 8 s, followed by a rest period of 10 s before the potentiated contraction (1). A second excitation was made after an additional 10-s rest period (2), and the sequence was repeated. The opposite baseline absorbance shifts at 470 and 580 nm caused by the potentiated contraction, taken together, are $\sim 30\%$ of the magnitude of the potentiated contraction artifacts at those wavelengths. The suppression of similar signals with citrate in both solutions was described previously (Hilgemann, 1986).

Fig. 11B shows the inverted 680-nm motion artifact at the potentiated contraction, the best estimate of the extracellular calcium transient (470–580 signal; average of five potentiated contraction signals), and the action potentials meas-

ured after the data acquisition period for the same sequence. The first action potential corresponds to a potentiated contraction; the second action potential corresponds to a subsequent excitation after an additional 10-s rest (see the numbers given in panel A; 680-nm signal). With a post-stimulatory rest period of 10 s, the initial repolarization of the first action potential can be nearly superimposed on that of the second action potential after an additional 10 s.

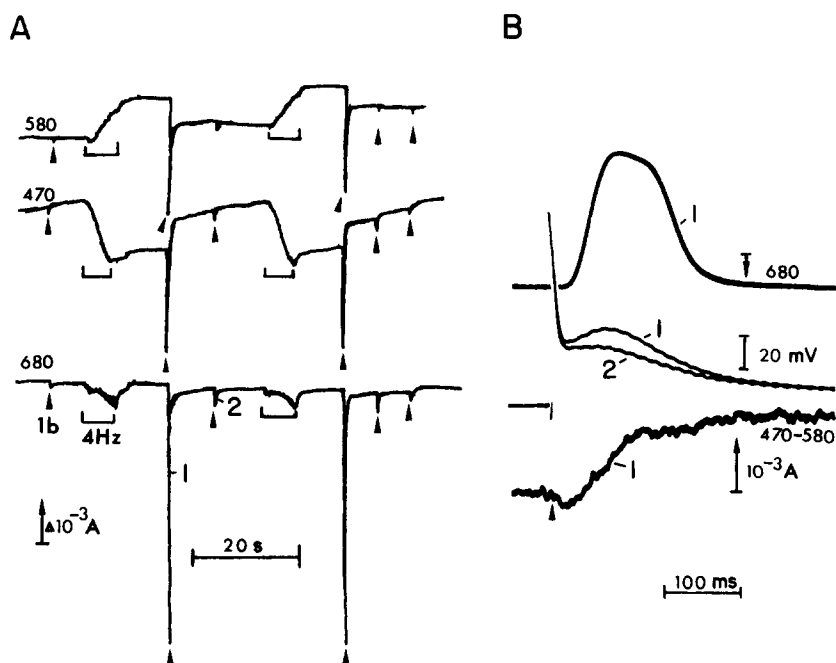


FIGURE 11. Extracellular calcium transient at potentiated post-stimulatory contraction. $150 \mu\text{M}$ total calcium. (A) Raw signals during the stimulation protocol: 4 Hz for 8 s, two stimulations at 10-s intervals, another 10 s rest, and then repetition of the sequence. Arrowheads correspond to the single stimulations. (B) Light signals for five averaged acquisitions at the first post-stimulatory excitation (marked "1" in A). The upper signal is the inverted 680-nm motion artifact. The lower signal is the best estimate of the extracellular calcium transient (470–580). The two action potentials given were measured after the data acquisition period, and correspond to the first and second post-stimulatory excitations in the stimulation sequence (marked in A). See text for complete details.

Repolarization did not detectably change with longer rest periods. The peak of the "hump" in the late action potential at the first excitation comes at -42 mV, and corresponds to a point just before the peak of contraction; the maximum potential difference between the two action potentials is 8 mV.

The extracellular calcium transient shows an initial small depletion phase of not more than $0.6 \mu\text{M}$. Net calcium accumulation reached a maximum rate within 25 ms, continued rapidly up to a point early in the relaxation of contraction, and continued through the terminal repolarization of the action potential in a slower phase. The signals reflect an estimated net increment of mean

extracellular calcium of $6 \mu\text{M}$. The difference between the two action potentials, corresponding to the potentiated contraction and the first small contraction thereafter, correlates very roughly with the time course of calcium efflux. The maximal rate of calcium accumulation was achieved well before the peak difference of the action potentials, and the rate of net accumulation decreased earlier than the difference between the two action potentials.

Fig. 12 relates the calcium transient at the potentiated contraction to those obtained for steady stimulation and paired pulse stimulation in the same preparation. The 680-nm motion artifacts are shown in part A; the 470–580 signals

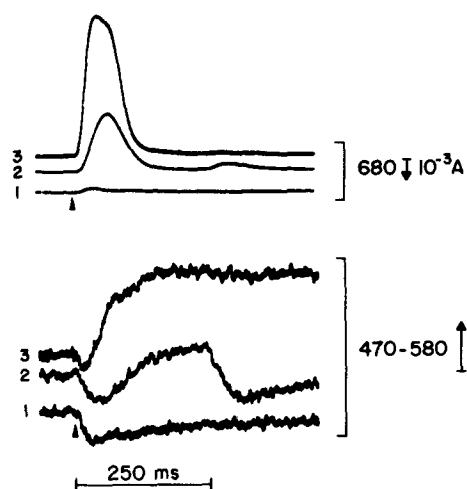


FIGURE 12. Extracellular calcium transients during steady state stimulation at 0.4 Hz (1), paired pulse stimulation at 250-ms intervals with basal frequency of 0.4 Hz (2), and at a potentiated post-stimulatory excitation 10 s after 4 Hz stimulation (3). Same muscle as Fig. 11 (five averagings). $150 \mu\text{M}$ total calcium. The upper signals are the 680-nm motion artifacts; the lower signals are the 470–580 signals. See text for further details.

are shown in part B. Signals labeled “1” are for steady 0.4 Hz stimulation; those labeled “2” are for paired stimulations at 300-ms intervals at 0.4 Hz basal frequency; those labeled “3” correspond to the potentiated contraction described in Fig. 9. The scaling factors are the same throughout. The calcium transient at 0.4 Hz is somewhat uncommon, since it shows almost no rapid replenishment phase. Note the increasing magnitude of the accumulation phase with paired stimulation and with the post-stimulatory potentiation. In this sequence, the very short duration of net depletion at the potentiated contraction can probably be accounted for by the very rapid repolarization after a 10-s rest period in comparison with the other transients with longer depletion phases.

Calcium Depletion at Post-Rest Stimulation in the Ryanodine State

It became apparent at an early point in this work that the large extracellular calcium depletions found at post-rest stimulation in ryanodine-pretreated muscles were related to a pronounced prolongation of depletion signals. Figs. 13 and 14

present results with $0.2 \mu\text{M}$ ryanodine pretreatment for 20 min during the equilibration period for the experiment. In Fig. 13, parts *A* and *B* are with $50 \mu\text{M}$ 4-AP, a concentration at which action potential staircases at post-rest stimulation accumulate in just two to four excitations and at which action potential upstrokes reach the same positive potential from one excitation to the next. Parts *C* and *D* are with 2 mM 4-AP. Part *A* shows the action potentials made at 250-ms intervals with a 20-s rest period. Repolarization at the first action potential is still quite rapid at this concentration of 4-AP, and the second action

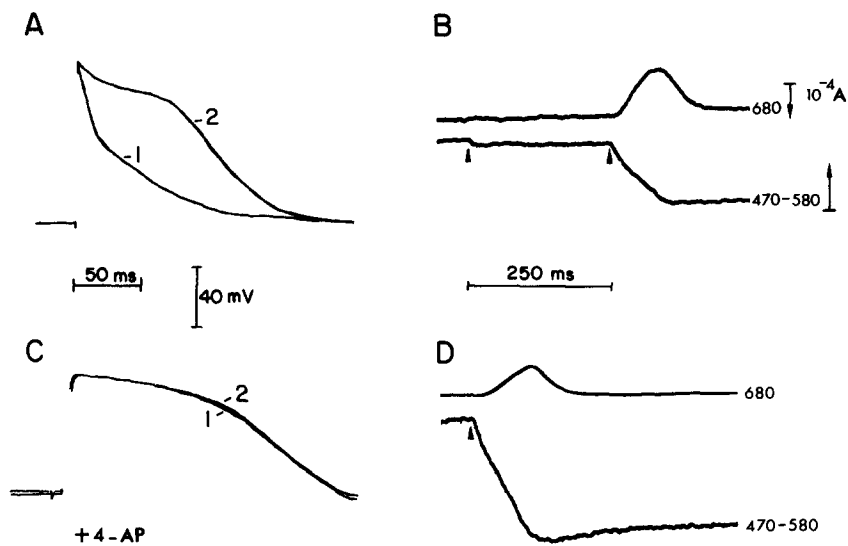


FIGURE 13. Action potentials and extracellular calcium transients at post-rest stimulation in the ryanodine state. $200 \mu\text{M}$ total calcium. (*A* and *B*) $50 \mu\text{M}$ 4-AP; (*C* and *D*) 2 mM 4-AP. Part *A* shows first two action potentials after a 20-s rest period; 250-ms intervals. Part *B* shows the 680-nm motion artifacts and calcium depletion signals for the same sequence, measured afterwards. Part *C* shows the first two action potentials for the same sequence after addition of 2 mM 4-AP, and *D* shows the 680-nm motion artifact and extracellular calcium transient for the first excitation. Note that the upstrokes of action potentials in *A* reach essentially the same final potential. See text for further explanations.

potential shows a prolonged plateau. Part *B* (note the slower time scale) shows the corresponding extracellular calcium transient (470–580 signal) and the 680-nm motion artifact record. At the first excitation, extracellular calcium depletion is small and brief (<10 ms); at the second excitation, the depletion is greatly prolonged and shows a gradual decrease of rate through the small contraction artifact. The initial depletion signals at the two excitations could be superimposed with appropriate display after further amplification.

Fig. 13 *C* shows the first two action potentials with 2 mM 4-AP, which are very prolonged for this preparation. Part *D* shows the corresponding extracellular calcium transient at the first excitation. The net extracellular calcium depletion continues through most of the small rested-state contraction with at most a 25%

reduction in rate over 130 ms. Although the initial rate of depletion here is not greater than that found routinely in rhythmically stimulated muscles, the total magnitude of depletion is >10 times greater. It is mentioned that the example chosen for presentation displayed the longest action potential of the preparations tested under these conditions (see preceding article for the behavior of depletion at subsequent excitations). It should be stressed that the length of the action potentials obtained in this circumstance is dependent on both ryanodine and 4-AP.

The reduction of the bath temperature to room temperature (24°C) was found

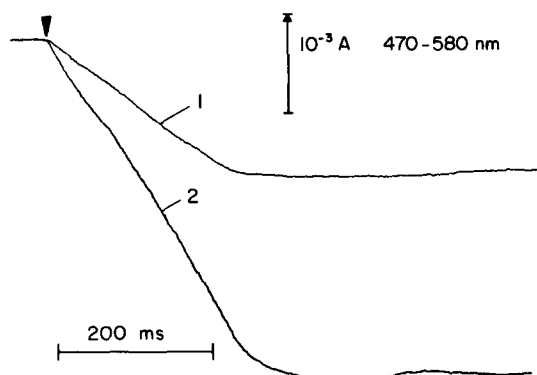


FIGURE 14. Extracellular calcium transients for post-rest stimulation in the ryanodine state at 24°C. 2 mM 4-AP. The depletion responses correspond to the first excitation after a 2-min rest period (20 averagings). Between the responses marked "1" and "2," 3×10^{-8} M isoproterenol was applied. Note the essentially linear depletion response in "1" and nearly linear response in "2" at roughly a twofold rate. See text for further explanations.

to routinely increase the action potential duration to >200 ms (not shown) under these conditions, and a typical extracellular calcium transient is shown in Fig. 14. Response number 1 shows the depletion found at the first excitation after a 2-min rest period. The depletion rate is estimated at $1.8 \mu\text{M}/10 \text{ ms}$ ($\sim 0.7 \mu\text{mol}/\text{kg wet weight} \cdot 10 \text{ ms}$, $200 \mu\text{M}$ total calcium, $120 \mu\text{M}$ free calcium) and the depletion continues almost linearly over >200 ms. Depletion response number 2 was obtained after addition of 3×10^{-8} M isoproterenol. The rate of depletion is increased by a factor of ~ 2 , and shows only small changes over 200 ms. The total magnitude of the depletion response is $\sim 12 \mu\text{mol}/\text{kg wet weight}$. It is worth noting that still larger, more prolonged depletion responses, up to 700 ms, have been obtained in perfused right ventricle of rabbit and cat under similar conditions and also showed little or no reduction in rate over the entire duration.

DISCUSSION

Are Extracellular Calcium Transients Adequately Resolved by the Subtraction Procedure?

The spectrophotometric resolution of extracellular calcium transients was first attempted under conditions predicted to result in the largest possible net calcium

influx with the smallest possible contraction; in fact, very substantial calcium depletions could be recorded in the complete absence of muscle contraction in mammalian heart (Hilgemann et al., 1983). Subsequently, experimental conditions were established under which net extracellular calcium shifts could be evaluated after the contractile event (Hilgemann and Langer, 1984*b*; Hilgemann, 1986). In the present work, the direct problem of muscle motion can also be avoided in drawing several conclusions. The initial depletion of extracellular calcium upon excitation begins well before onset of the motion signal, and at premature excitations, net calcium depletion can often be recorded with almost no contraction artifact. The precise subtraction of the contraction artifact does not affect the conclusion that replenishment of extracellular calcium can be almost complete by the end of relaxation in a rhythmically stimulated muscle. At potentiated contractions, the net accumulation of extracellular calcium is placed unambiguously in the time frame between the onset and end of the motion signal; as stressed throughout the Results, this time course is the aspect most strongly influenced by the motion subtraction. In Fig. 9, the subtraction procedure favored nearly the fastest possible time course of net calcium accumulation at the initial contraction in a quadruple pulse sequence. In Fig. 7 (result number 3), the subtraction procedure favored nearly the slowest possible time course of calcium accumulation at the initial contraction in a paired pulse sequence. Even allowing for the greatest possible error in determining these time courses, the rate of net extracellular calcium accumulation at highly potentiated contractions is in the range of the initial rate of net depletion. The wavelength independence of motion signals under precisely the optical conditions of experiments has been established, and the suppression of the calcium-dependent signal components with citrate is a specific and independent means of subtracting the contraction component. Thus, future methodological refinements may well improve on the ratio of calcium-dependent to contraction-dependent signals, but major revisions of the time courses given do not appear to be possible.

Extracellular Calcium Transients During Steady State and Non-Steady State Stimulation

The very rapid onset of extracellular calcium depletion at excitation (2–4 ms) is fully comparable to the fast activation kinetics of calcium channels found in cardiac myocytes (e.g., Isenberg and Kloeckner, 1982; Mitchell et al., 1983; Lee and Tsien, 1984). This rapidity is also consistent with calcium electrode records of extracellular calcium depletion (Bers, 1983), although maximal depletions were not attained within 4–8 ms of excitation here, as appears to be the case in electrode signals. For the development of the spectrophotometric methodology, the present results demonstrate that tetramethylmurexide is in rapid equilibrium with free extracellular calcium at membrane surfaces. The finding of almost complete re-equilibration of extracellular calcium within the contraction during regular stimulation is different from extracellular calcium transients determined in frog ventricle (Cleeman et al., 1984; Hilgemann and Langer, 1984*a*; Dresdner and Kline, 1985), where a slow replenishment of extracellular calcium has been found over the course of many seconds between excitations. However, frog

ventricle does show a small rapid phase of extracellular calcium accumulation at the onset of relaxation (see records of Cleeman et al., 1984), which becomes substantially larger at high frequencies of contraction (0.6–1 Hz; Hilgemann and Langer, 1984a). Neither in the present work nor in any of the records cited has net extracellular calcium accumulation been observed at positive potentials. In rabbit atrium, the inferred efflux of calcium during contraction must be accounted for within the later portion of the action potential in a negative potential range (e.g., Fig. 3).

The time courses of net extracellular calcium depletion and replenishment during steady stimulation are consistent with at least some contribution of sarcolemmal mechanisms to the activation and relaxation of contraction in this preparation. However, a relative contribution of calcium influx to activation cannot be proposed, since during non-steady state stimulation and with pharmacological intervention, calcium depletion can be completely dissociated from contractile activity. The present work clearly favors a facilitation of calcium influx as an important mechanism of frequency inotropy in this preparation; prolongation of net depletion responses with an increase of frequency (Figs. 7 and 13) is consistent with action potential broadening as the primary mechanism (Hilgemann, 1986), rather than factors determining early calcium influx (e.g., calcium channel conductance). In multicellular preparations, the recovery of calcium current after an excitation was sometimes found to parallel the recovery of contractility (see Noble, 1984, for review) and was sometimes found to precede the recovery of contractility (e.g., Gibbons and Fozzard, 1975). The present work demonstrates strikingly that calcium influx can be activated fully within 200–250 ms of a previous excitation at a time when recovery of contractility (“restitution”) has just begun.

As pointed out in the Results, the termination of calcium depletion could be determined by repolarization, overlap of calcium efflux with calcium influx, or inactivation of calcium channels. At least at potentiated contractions in the presence of 4-AP, extracellular calcium depletion does stop at relatively positive potentials (about -10 mV), and the subsequent rate of calcium accumulation is slow enough to suggest inactivation (Fig. 8). The finding of prolonged depletion at premature excitations, and the almost undiminished depletion for >200 ms in the ryanodine state (Figs. 13 and 14), suggest that the voltage protocol of an action potential alone does not support significant inactivation. Even at enhanced rates of depletion with isoproterenol, depletion can continue almost linearly over 200 ms (Fig. 14). The probable explanation at present is that initiation of calcium channel inactivation by calcium (Eckert and Tillotson, 1981; see Eckert and Chad, 1984, for review) depends on calcium release in mammalian heart, internal calcium uptake being sufficiently fast to prevent substantial cytosolic calcium accumulation in this preparation. The prolongation of calcium currents by ryanodine in rat myocytes (Mitchell et al., 1984) supports this interpretation (see also the discussion of Marban and Weir, 1985). However, the duration of the depletions described here would not be accounted for by these currents. As an explanation, the low calcium concentrations used in the present measurements could well be expected to forestall inactivation. At potentiated contractions, an

early termination of calcium current would favor a more rapid initial repolarization, which would be found even with high concentrations of 4-AP (Fig. 8; see also Fig. 4 of Hilgemann, 1986). The early activation of an outward current associated with calcium release would be a likely additional explanation (Siegelbaum and Tsien, 1980; Kenyon and Sutko, 1985).

The very prolonged depletions found under specific conditions appear to eliminate a role of calcium depletion in restricted spaces in the normal termination of calcium influx, which is probably much faster. This conclusion is also supported by the fact that contractility in highly buffered calcium solutions is not greater, but usually somewhat smaller, than in control solutions of the same pCa. The same conclusion was reached on the basis of a voltage-clamp analysis of calcium current in a multicellular preparation (Kass and Sanguinetti, 1984). Up to now, the only circumstance in which extracellular calcium transients favor a restriction of calcium influx by depletion is during multiple rapid post-rest stimulations in the ryanodine state (Hilgemann, 1986). An extremely rapid depletion at the mouth of calcium channels, which would be a determinant of permeation but not current time courses, remains a possibility.

Throughout the results presented here, calcium efflux is enhanced as the contractile state is enhanced by premature or rapid excitations. At the earliest, net extracellular calcium accumulation begins with the onset of the motion signal (Figs. 9–12). Therefore, it seems reasonable to suggest that calcium appearing in the extracellular space passed through the cytosol and was extruded by the sarcolemma after contributing to activation. An alternative suggested by various authors, with different formulations, was that calcium efflux at activation could take place through “feet” or junctions of sarcoplasmic reticulum with the sarcolemma. (*a*) A specialized calcium store in communication with the extracellular space would take up calcium after release from another store and allow a subsequent outflow (Wohlfart, 1979). (*b*) Calcium movement through couplings would begin essentially instantaneously with excitation and provide an extracellular source of stored calcium for influx mechanisms (Mensing and Hilgemann, 1981). (*c*) Calcium released internally would reach high enough concentrations in diffusion-restricted junctional areas to allow a movement to the extracellular space (Maylie and Morad, 1984). The net extracellular calcium accumulations described in the present work are clearly not compatible with those mechanisms, which would make calcium efflux voltage dependent in the sense of stimulation by depolarization. Rather, potentiated post-rest contractions of rabbit atrium with a spike-like repolarization appear to present optimal conditions for efflux, and fast efflux rates at potentials of less than -40 mV (Fig. 11) are consistent with sodium-calcium exchange. Net extracellular calcium accumulation begins at an early enough point in time to explain a more positive late action potential by sodium-calcium exchange. Terminal repolarization would be determined both by the magnitude of outward current and the decay of exchange current.

The finding of complex time courses of extracellular calcium accumulation (e.g., Fig. 10) could be suggestive of multiple mechanisms, and no available data discount a significant sarcolemmal calcium pump role. However, several factors could result in a complicated efflux time course through a single mechanism.

The rapid phase of calcium efflux, found under most circumstances between the initial rise and the peak of motion signals, would correspond reasonably to the relaxation of intracellular calcium transients measured with aequorin (e.g., Marban and Wier, 1985). Late components of calcium efflux during the contraction (Figs. 3, 4, 7, 9, and 10) could, for example, be related to removal of calcium from binding sites with a slow off rate.

Integrated Function of Sarcolemmal Mechanisms and Corresponding Quantitative Considerations

The present results complement in many respects the recent calcium release experiments of Fabiato (1985*a, b*) in skinned cardiac cells, which would define the mechanistic role of the sarcoplasmic reticulum in post-stimulatory potentiation and paired pacing as follows. Early excitations result in contractions of very small magnitude because they fall upon an inactivated calcium release mechanism and because calcium uptake by the store does not permit activation except by a very rapid calcium release. Calcium efflux would correspond to diffusion of calcium to the surrounding solution and its subsequent aspiration. As outlined in this discussion and by Fabiato, the primary physiological determinants, apart from a calcium-dependent release mechanism, would be a fast calcium channel and a fast electrogenic sodium-calcium exchanger. Under the conditions of the present experiments in rabbit atrium, the kinetic behavior of these mechanisms appears to be remarkably similar to the physical determinants in calcium release experiments (e.g., potentiation decays in just two to three excitations). Since the original version of this manuscript was written, the viability of this interpretation has been demonstrated by simulation of the fast extracellular calcium transients in detail with precisely these assumptions (refinements of the DiFrancesco-Noble [1984] model of cardiac electrical activity in Hilgemann and Noble, 1985).

Assuming a sodium-calcium exchange ratio of 3:1, the rates of net extracellular calcium depletion and accumulation might quantitate roughly the relative magnitudes of calcium current and sodium-calcium exchange current during excitation. At potentiated contractions with a rapid initial repolarization in the present work, the extracellular calcium accumulation rates are clearly in the general range of the initial depletion rates. This would suggest the presence of sodium-calcium exchange currents of very roughly one-half the magnitude of calcium currents under optimal conditions for calcium efflux. During steady stimulation, the extracellular calcium transients would project only small exchange currents, since the apparent rates of calcium accumulation are much smaller than the initial rates of calcium depletion. The basic predictions from extracellular calcium transients were remarkably consistent with the original simulations of DiFrancesco and Noble (1984).

The assumed involvement of sodium-calcium exchange in calcium extrusion predicted a calcium-dependent sodium load under physiological conditions even with a 2:1 stoichiometry, and the expected magnitudes of sodium movements are of fundamental importance to an understanding of sodium homeostasis. In the present work, the magnitude of net calcium influx, assuming no overlap of depletion and accumulation, is $\sim 0.3 \mu\text{mol/kg}$ wet weight with $135 \mu\text{M}$ free

calcium. If the relation of calcium influx to extracellular calcium were linear, an influx of $5 \mu\text{mol/kg}$ wet weight would be expected with 2 mM external calcium (less than one-half the estimate of Bers, 1983; an order of magnitude smaller than the steady state estimate of Pytkowski et al., 1983). Accordingly, a sodium influx by the exchanger of $15 \mu\text{mol/kg}$ wet weight per contraction cycle would be expected, assuming for the sake of argument that all calcium influx is via calcium channels and all efflux is via a 3:1 exchanger. That would be substantially more sodium influx than needed for an action potential upstroke, and, at least in Purkinje fibers, the bulk of available data does not appear to support the prediction (see, e.g., January and Fozzard, 1984, for tetrodotoxin sensitivity of sodium loading; see Ellis, 1985, for a recent estimation of activation-dependent sodium influx at just the minimum needed for upstroke; and see Falk and Cohen, 1984, for indirect evidence of a calcium-dependent sodium load using a high-frequency voltage-clamp protocol with an estimation of sodium load from post-stimulatory "overdrive" currents). Although large background sodium conductances appear to complicate the estimation of sodium influx during depolarization in Purkinje fibers (e.g., Ellis, 1985), substantial quantitative problems are also apparent in other types of data from other preparations. As a recent example, the exemplary calcium current given by Fabiato (1985*b*), and provided by R. D. Tsien, projects over its first 125 ms to a calcium influx of $\sim 40 \mu\text{mol/liter}$ cell after integration (guinea pig ventricular myocyte with EGTA, 5 nA peak current, and an assumed cell volume of 50 pl). Highly activated sodium pump currents in guinea pig myocytes (Gadsby et al., 1985) project to $\sim 7 \text{ mM}$ sodium extrusion/liter cell \cdot min (120-pA currents at high temperature and 34 mM internal sodium). If the exemplary calcium current were representative of physiological currents, the sodium pump would saturate from sodium influx by the exchanger alone at a frequency of just more than 1 Hz; a square wave of calcium current over 25 ms at 5 nA would saturate the pump at 2 Hz.

One conceivable solution would be that calcium current magnitudes measured in isolated myocytes are not representative of intact muscle. However, the present work is indeed consistent with myocyte calcium current magnitudes; calcium influx of $0.2 \mu\text{mol/kg}$ wet weight \cdot 10 ms at $135 \mu\text{M}$ free calcium would correlate with a 5-nA calcium current in a 50-pl cell at just over 2.5 mM external calcium, assuming a linear calcium-current relationship (35% extracellular space; if average atrial cell volumes are substantially less than 50 pl, then current magnitudes would be correspondingly smaller). The remaining possibility is that a very rapid inactivation of calcium current by intracellular calcium release limits calcium influx to the very early portions of the mammalian cardiac action potential and thereby limits greatly the potential calcium-dependent sodium pump load. This possibility is tentatively supported by the present work, which projects to the smallest calcium influx estimate of all recent methodological approaches at physiological rates. At physiological calcium concentrations, calcium influx would be expected to be still more brief than expected from extracellular calcium transients at low calcium. Clearly, a great deal of quantitative experimentation will be necessary to test this possibility, as well as alternatives that would allow a less tight coupling of calcium and sodium movements in excitation-contraction coupling.

The author is very indebted to Dr. Glenn A. Langer for his support and personal encouragement of this work over the last three years. Drs. Glenn A. Langer and Bernard Ribalet are gratefully acknowledged for their helpful comments on the first version of this manuscript, Dr. Michael Barish for his generous loan of equipment, and Victor Cordoba for his expert computer assistance.

This work was supported by the Laubish Foundation and by an award to the author as a George and Edna Lievre Family Research Fellow. The author is a Senior Investigator of the American Heart Association, Greater Los Angeles Affiliate.

Large portions of the work described here were presented at the 1985 Biophysical Society Meeting (Hilgemann, 1985).

Original version received 10 June 1985 and accepted version received 26 November 1985.

REFERENCES

- Anderson, T. W., C. Hirsch, and F. Kavalier. 1977. Mechanism of activation of contraction in frog ventricular muscle. *Circulation Research*. 41:472-480.
- Antoni, H., R. Jakob, and R. Kaufmann. 1969. Mechanische Reaktionen des Frosch- und Säugetiermyokards bei Veränderung der Aktionspotential-Dauer durch konstante Gleichstromimpulse. *Pflügers Archiv European Journal of Physiology*. 306:33-57.
- Bers, D. M. 1983. Early transient depletion of extracellular Ca during individual cardiac muscle contractions. *American Journal of Physiology*. 244:H462-H468.
- Bowditch, H. P. 1871. Über die Eigenthümlichkeiten der Reizbarkeit, welche die Muskelfasern des Herzens zeigen. *Arbeiten Physiologisches, Anstalt, Leipzig*. 6:139-176.
- Boyett, M. R. 1981. Effect of rate-dependent changes in the transient outward current on the action potential in sheep Purkinje fibres. *Journal of Physiology*. 319:23-41.
- Brown, H. F., J. Kimura, D. Noble, S. J. Noble, and A. Taupignon. 1984. The slow inward current in the rabbit sino-atrial node investigated by voltage clamp and computer simulation. *Proceedings of the Royal Society of London B Biological Sciences*. 222:305-328.
- Cleeman, L., G. Pizarro, and M. Morad. 1984. Optical measurements of extracellular calcium depletion during a single heartbeat. *Science*. 226:174-177.
- Cohen, C. J., H. A. Fozzard, and S.-S. Sheu. 1982. Increase in intracellular sodium ion activity during stimulation in mammalian cardiac muscle. *Circulation Research*. 50:651-662.
- Cranefield, P. F., and B. F. Hoffman, editors. 1968. Paired Stimulation of the Heart. Proceedings of the Second Conference on Paired Pulse Stimulation and Postextrasystolic Potentiation in the Heart. The Rockefeller University Press, New York.
- Dani, J. A., J. A. Sanchez, and B. Hille. 1983. Lyotropic anions. Na channel gating and Ca electrode response. *Journal of General Physiology*. 81:255-281.
- DiFrancesco, D., and D. Noble. 1984. A model of cardiac electrical activity incorporating ionic pumps and concentration changes. *Philosophical Transactions of the Royal Society of London*. 307:353-398.
- Dresdner, K. P., and R. P. Kline. 1985. Extracellular calcium ion depletion in frog ventricular muscle. *Biophysical Journal*. 48:33-46.
- Eckert, R., and J. E. Chad. 1984. Inactivation of calcium channels. *Progress in Biophysics and Molecular Biology*. 44:215-267.
- Eckert, R., and D. Tillotson. 1981. Calcium-mediated inactivation of the calcium conductance in cesium-loaded giant neurones of *Aplysia californica*. *Journal of Physiology*. 314:265-280.
- Ellis, D. 1985. Effects of stimulation and diphenylhydantoin on the intracellular sodium activity in Purkinje fibres of sheep heart. *Journal of Physiology*. 362:331-348.
- Fabiato, A. 1985a. Time and calcium dependence of activation and inactivation of calcium-

- induced release of calcium from the sarcoplasmic reticulum of a skinned canine cardiac Purkinje cell. *Journal of General Physiology*. 85:247–289.
- Fabiato, A. 1985b. Simulated calcium current can both cause calcium loading in and trigger calcium release from the sarcoplasmic reticulum of a skinned canine cardiac Purkinje cell. *Journal of General Physiology*. 85:291–320.
- Falk, R. T., and I. S. Cohen. 1984. Membrane current following activity in canine cardiac Purkinje fibers. *Journal of General Physiology*. 83:771–799.
- Gadsby, D. C., J. Kumura, and A. Noma. 1985. Voltage dependence of Na/K pump current in isolated heart cells. *Nature*. 315:63–65.
- Gibbons, W. R., and H. A. Fozzard. 1975. Slow inward current and contraction of sheep cardiac Purkinje fibers. *Journal of General Physiology*. 65:367–384.
- Grossman, A., and R. R. Furchgott. 1964. The effects of frequency of stimulation on Ca-45 exchange and contractility on the isolated guinea pig auricle. *Journal of Pharmacological and Experimental Therapeutics*. 143:120–130.
- Hilgemann, D. W. 1985. Extracellular calcium transients at single excitations in rabbit atrium. *Biophysical Journal*. 47(2, Pt. 2):376a. (Abstr.)
- Hilgemann, D. W. 1986. Extracellular calcium transients and action potential configuration changes related to post-stimulatory potentiation in rabbit atrium. *Journal of General Physiology*. 87:675–706.
- Hilgemann, D. W., M. Delay, and G. A. Langer. 1983. Activation-dependent cumulative depletions of extracellular free calcium in guinea pig atrium measured with antipyrilazo III and tetramethylmurexide. *Circulation Research*. 53:779–793.
- Hilgemann, D. W., and G. A. Langer. 1984a. Extracellular calcium transients in frog ventricle measured with antipyrilazo III and tetramethylmurexide. *Federation Proceedings*. 43:3130. (Abstr.)
- Hilgemann, D. W., and G. A. Langer. 1984b. Transsarcolemmal calcium-movements in arterially perfused rabbit right ventricle measured with extracellular calcium-sensitive dyes. *Circulation Research*. 54:461–467.
- Hilgemann, D. W., and D. Noble. 1986. Simulation of extracellular transients in rabbit cardiac muscle. *Journal of Physiology*. 371:195P. (Abstr.)
- Isenberg, G., and U. Klockner. 1982. Calcium currents in bovine ventricular myocytes are fast and of large amplitude. *Pflügers Archiv European Journal of Physiology*. 395:30–42.
- January, C. T., and H. A. Fozzard. 1984. The effects of membrane potential, extracellular potassium, and tetrodotoxin on the intracellular sodium ion activity of sheep cardiac muscle. *Circulation Research*. 54:652–665.
- Kass, R. S., and M. C. Sanguinetti. 1984. Inactivation of calcium channel current in the calf cardiac Purkinje fiber. Evidence for voltage- and calcium-mediated mechanism. *Journal of General Physiology*. 84:705–726.
- Kavaler, F. 1974. Electromechanical time course in frog ventricle: manipulation of calcium level during voltage clamp. *Journal of Molecular and Cellular Cardiology*. 6:575–580.
- Kenyon, J. L., and J. L. Sutko. 1985. Ryanodine and aminopyridine sensitive currents of cardiac Purkinje fibers. *Biophysical Journal*. 47(2, Pt. 2):498a. (Abstr.)
- Langer, G. A. 1984. Calcium at the sarcolemma. *Journal of Molecular and Cellular Cardiology*. 16:147–153.
- Langer, G. A. 1985. The effect of pH on cellular and membrane calcium binding and contraction of myocardium: a possible role for sarcolemmal phospholipid in EC coupling. *Circulation Research*. 57:374–382.

- Lee, K. S., and R. W. Tsien. 1984. High selectivity of calcium channels in single dialysed heart cells of the guinea pig. *Journal of Physiology*. 354:253–272.
- Marban, E., and W. G. Wier. 1985. Ryanodine as a tool to determine the contributions of calcium entry and calcium release to the calcium transient and contraction of cardiac Purkinje fibers. *Circulation Research*. 56:133–138.
- Maylie, J., and M. Morad. 1984. A transient outward current related to calcium release and development of tension in elephant seal atrial fibres. *Journal of Physiology*. 357:267–292.
- McLaughlin, A., W.-K. Eng, G. Vaio, T. Wilson, and S. McLaughlin. 1983. Dimethonium, a divalent cation that exerts only a screening effect on the electrostatic potential adjacent to negatively charged phospholipid bilayer membranes. *Journal of Membrane Biology*. 76:183–193.
- Mensing, H. J., and D. W. Hilgemann. 1981. Inotropic effects of activation and pharmacological mechanisms in cardiac muscle. *Trends in Pharmacological Sciences*. 2:303–307.
- Mitchell, M. R., T. Powell, D. A. Terrar, and V. W. Twist. 1983. Characteristics of the second inward current in cells isolated from rat ventricular muscle. *Proceedings of the Royal Society B Biological Sciences*. 219:447–469.
- Mitchell, M. R., T. Powell, D. A. Terrar, and V. W. Twist. 1984. Ryanodine prolongs Ca-currents while suppressing contraction in rat ventricular muscle cells. *British Journal of Pharmacology*. 81:13–15.
- Morad, M., Y. E. Goldman, and D. R. Trentham. 1983. Rapid photochemical inactivation of Ca²⁺-antagonists shows that Ca²⁺ entry directly activates contraction in frog heart. *Nature*. 304:635–638.
- Noble, D. 1984. The surprising heart: a review of recent progress in cardiac electrophysiology. *Journal of Physiology*. 353:1–50.
- Noble, S., and Y. Shimoni. 1981. Voltage-dependent potentiation of the slow inward current in frog atrium. *Journal of Physiology*. 310:77–95.
- Pytkowski, B., B. Lewartowski, A. Prokopczuk, K. Zdanowski, and K. Lewandowska. 1983. Excitation- and rest-dependent shifts of Ca in guinea-pig ventricular myocardium. *Pflügers Archiv European Journal of Physiology*. 398:103–113.
- Siegelbaum, S. A., and R. W. Tsien. 1980. Calcium-activated outward current in calf cardiac Purkinje fibres. *Journal of Physiology*. 299:485–506.
- Winegrad, S., and A. M. Shanes. 1962. Calcium flux and contractility in guinea pig atria. *Journal of General Physiology*. 45:371–394.
- Wohlfart, B. 1979. Relationships between peak force, action potential duration and stimulus interval in rabbit myocardium. *Acta Physiologica Scandinavica*. 106:395–409.